

## SOLID EARTH MODELLING PROGRAMME

*Solid Earth Modelling Programme (SEMP) research focuses on integration of GPS, computational seismology, tectonics, geology and ground motion modeling for quantification of natural hazard (Earthquake, Landslides, Extreme Events) specific to Indian subcontinent. This is a multidisciplinary and multi-component research programme including Engineering and Earth Sciences. In this year we have successfully completed the milestones of DREAMS (Data intensive Research for Earthquake hazard Assessment by Modelling the Solid earth) as a part of CSIR 12<sup>th</sup> FYP project ARiEES. Our work component was highly commended by Sectorial Monitoring Committee and recommended as Knowledge Product Lead for further research. Our group has 7 SCI publications in High Impact factor journals and about 220 citations during 2016-17. For the first time accuracy of SRTM heights in the Indian subcontinent were evaluated using GPS heights of about 200 GPS points. Comprehensive study of crustal models and water vapor for Northeast India using 12 years of GPS observations gave significant insights in to the tectonic deformation, spatial and temporal variability of atmospheric water vapor and its relation to the observed rainfall. We have established 2 new CGNSS stations and re-measured campaign sites in Northeast India and Gharwal Himalayas. We operated and maintained the broadband seismic and GNSS network in Kashmir Himalayas and first ever crustal and mantle structure in the Kashmir Himalaya has been reported. In addition, the site specific microzonation of Srinagar city has been initiated and micro tremor data have been acquired and analyzed. The Neo-Deterministic seismic hazard map for the entire country has been prepared and published.*

### **Inside**

- *Evaluation of SRTM heights using GPS heights for Indian subcontinent*
- *Estimation of Euler pole of rotation of Shillong plateau-Assam valley and crustal deformation models for northeast India*
- *Multi-scale variability of GPS-PWV in northeast India and correlation with rainfall*
- *Estimation of PWV and TEC from 12 years of GPS observations*
- *Active deformation studies in northeast India*
- *Active crustal deformation and landslide studies in Garhwal Himalayas*
- *Establishment, operation and maintenance of continuous mode Global Navigation Satellite System (CGNSS) stations*

- *Crustal deformation studies using CGNSS network in Kashmir Valley*
- *Landslide mitigation studies in Uttarakhand and northeast India*
- *Seismic hazard and risk assessment based on the Unified Scaling Law for Earthquakes: Thirteen Principal Urban Agglomerations of India*
- *Crustal structure of the Kashmir Basin in northwest Himalaya*
- *Strong ground motion estimation in northwest Himalaya using stochastic finite-fault method*
- *Ambient Noise Tomography of the Kashmir Basin: Cross-correlations of daily waveforms*
- *Earthquake catalogue in north Himalaya for hazard analysis in Jammu & Kashmir*
- *Receiver function interpolation computation for central Himalaya*
- *Site Characterization of Srinagar City, Kashmir Valley, Northwest Himalaya H/V spectral ratio method*
- *Subsurface profiling along Banni Plains and bounding faults, Kachch, Western India using Micro tremors method*
- *Subsurface profiling of granite pluton using micro tremor method: southern Aravalli, Gujarat, India*
- *A study on Progressive Collapse behaviors' of steel and RCC moment frames*
- *Study on special truss moment frames and special moment resisting frames with fluid viscous dampers as a seismic retrofit*
- *Study on P-delta effects of a building with soft storey*
- *Dynamic analysis to compare buckling restrained braces and conventional braces in RC frames*

## **5.1 Evaluation of SRTM heights using GPS heights for Indian subcontinent**

For the first time Vertical Heights of the Shuttle Radar Topography Mission (SRTM) Digital Terrain Elevation Data (DTED) are evaluated using new data from ~200 high-precision static Global Position System (GPS) ICPs in Indian subcontinent. Study indicates that only 1-arc X-Band data are usable "as is" in the Himalaya as it has height accuracy of 9.18m (RMSE). In contrast, "as-is" 1- and 3-arc C-Band have a height accuracy of RMSE 23.53m and 47.24m respectively and need to be corrected before use. Outlier and void filtering improves the height accuracy to RMSE 8m, 10.14m, 14.38m for 1-arc X and C-Band and 3-arc C-Band data respectively. Correction of the positive mean bias of the C-Band data is essential to get their accuracy within the SRTM goal of minimum vertical accuracy of 16m absolute error at 90% confidence (equivalent Root Mean Square Error (RMSE) of 9.73m) world-wide. The accuracy of the SRTM data in the Himalaya decreases with increase in elevation for all SRTM Digital Terrain Elevation Data. Consequently, we find that the SRTM heights in the Himalayan foreland are most accurate followed by the foothills. The Higher Himalaya heights have the least accuracy. Overall X-Band SRTM heights appear to be most accurate and should be preferred over C-Band wherever available. In the absence of X30, the recently released C30 should be used. The C90 data does not comply with the SRTM goal and is the most inaccurate everywhere. For effective use of SRTM data, it is required to re-sample the original DEM to a higher resolution and removing the mean error bias. All the bands of SRTM data showed a positive mean bias and correcting this significantly improved the accuracy of all the SRTM DEMs. Hence an initial assessment, re-sampling and mean correction is a quick and an effective way of improving the quality of the DTED before its use to obtain statistically meaningful insights from SRTM heights.

## **5.2 Estimation of Euler pole of rotation of Shillong plateau-Assam valley and crustal deformation models for northeast India**

The Euler pole of rotation of this central Shillong Plateau-Assam Valley (SH-AS) block is estimated using active deformation rates from 11years (2002-2013) of GPS observations. SH-AS block rotation pole is located at  $-25.1 \pm 0.2^\circ$  N,  $-97.8 \pm 1.8^\circ$  E and the estimated angular velocity is  $0.533 \pm 0.10^\circ$  Myr<sup>-1</sup> relative to India-fixed reference frame. Crustal deformation models of Kopili fault located between Shillong Plateau and Mikir massif, estimate a dextral slip of  $4.7 \pm 1.3$  mm/yr with a locking depth of  $10.2 \pm 1.4$  km indicating the fragmentation of Assam Valley across the fault. Presently, western edge of Mikir massif appears to be locked to Assam block indicating strain accumulation in this region. First order elastic dislocation modeling of the GPS velocities estimate a slip rate of 16 mm/yr along the Main Himalayan Thrust in Eastern Himalaya which is locked over a width of 130 km from the surface to a depth of 17 km with under thrusting Indian plate. Around ~9 mm/yr arc-normal convergence is accommodated in Lesser Himalaya just south of Main Central Thrust indicating high strain accumulation. Out of 36 mm/yr (SSE) India-Sunda plate motion, about ~16 mm/yr motion is accommodated in Indo-Burmese Fold and Thrust Belt, both as normal convergence (~6 mm/yr) and active slip (~7-10 mm/yr) in this region.

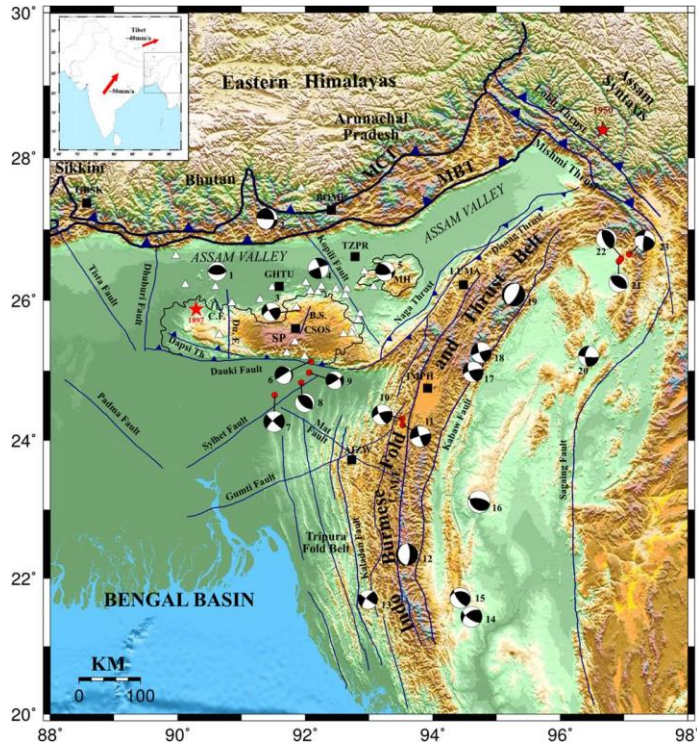


**Figure 5.1** Tectonic setting of Northeast India with GPS continuous (Black rectangles) and campaign (white triangles) stations

The focal mechanism solution of the earthquakes occurring along the Indo-Burmese accretionary wedge (Figure 5.1) indicates strike-slip faulting and north-south shortening parallel to the eastern margin of the Indian plate. This oblique convergence of India-Sunda plate along the Indo-Burmese arc, absorbed by the strike-slip movement as shown by our study, indicates reduced potential for future tsunamigenic earthquakes in the Northern Bengal Basin. Further should an earthquake occur in this region, the thick sediments of the Bengal fan will contribute towards reduction of the amplitude of the seismic waves as demonstrated by numerical models in this region.

### 5.3 Multi-scale variability of GPS-PWV in northeast India and correlation with rainfall

We present multi-scale variability of GPS derived column integrated Precipitable Water Vapour (PWV) estimated over five continuous GPS sites of northeast India from 2004 to 2012 (Figure 5.2) The average PWV for the study period is ~ 17 mm at Bomdila in the Eastern Himalayas, ~ 20 mm at Shillong in Shillong plateau, ~ 31 mm at Lumami in Arokan-Yoma Hill ranges, ~ 43 mm at Guwahati and Tezpur in Assam valley. The high altitude sites shows low annual PWV variability (~49%) than the low altitude sites (~63-67%). Seasonal PWV value coincides with the monsoon with maximum in summer and minimum in the winter. However, percentage seasonal PWV variability is found to be almost same (~68%) for all the five sites. Seasonal PWV cycle is a result of several processes and depends on the relation between multiple factors like moisture transport, convection, surface evaporation fluxes and humidity in the atmospheric column specific to a region. The Assam valley sites do not show a distinct diurnal cycle whereas the high altitude sites indicate a distinct diurnal cycle coinciding with the daily solar cycle. Absence of distinct diurnal cycle in Assam valley may be due to local wind flow pattern and condensation as these sites are located very close to river Brahmaputra and have extremely wet seasons throughout the year. TRMM derived rainfall follows the PWV variability pattern at TZPR and BOMP sites in northeast India over a 9 year period with maximum in summer with the arrival of the summer monsoon and PWV also reaches its extreme at the same time. The threshold PWV for high intensity rainfall is 54 mm for the TZPR site located in Assam Valley and 32 mm for high altitude Bomdila site located

in eastern Himalayas. The variation of monthly average PWV with measured monthly rainfall at TZPR site over a six year period, indicates close relation between PWV variability and the actual precipitation. The rainfall pattern over a region is a result of complex interaction between various atmospheric factors like water vapour and its transport, orography, vegetation, solar insolation, atmospheric instability etc. The observed rainfall variation with PWV need to be further studied considering all these parameters for better understanding the rainfall process prevailing in northeast India. Nevertheless, current study presents a firsthand comparison of GPS derived PWV with rainfall and point out the direction and importance of further study. The PWV values can be useful for understanding the weather formation and evaluation process of northeast India. The same PWV estimates can be assimilated into weather models for improvement of weather prediction which will be beneficial to the agrarian society of northeast India.

#### 5.4 Estimation of PWV and TEC from 12 years of GPS observations

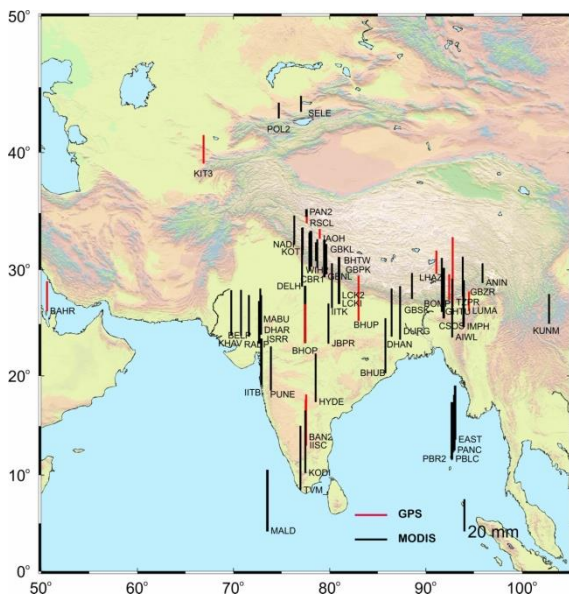


Figure 5.2 Measured PWV column for a 12 year period (2001-2013)

Precipitable Water Vapour (PWV) in atmosphere and Total Electron Content (TEC) in ionosphere is estimated using continuous Global Positioning System observations from 2001-2013 at ~55 locations spatially spread over Indian subcontinent. Multi-scale variability of PWV and TEC over the Indian subcontinent give significant insights in to the causative factors and processes such as moisture transport, convection, surface evaporation fluxes, humidity in the atmospheric column specific to a region, solar insolation, diurnal variations in moist convection and precipitation, surface wind convergence, surface evapo-transpiration, equatorial effects, ionospheric anomalies and their relation with seismic activity etc. Total integrated water vapour column for Indian subcontinent for the 12 year period is given in Figure 5.2

#### 5.5 Active deformation studies in north-east India

The entire North-East India (Figure 5.1) is one of the most seismically active regions in the Himalayas and falls under Zone-V. This area is wedged between the northern Indo-Tibetan collision zone and the eastern Indo-Burman collision boundary. The north-east India region is a spur (piece of land) of Precambrian crystalline basement, exposed over a large area in the Shillong plateau and Mikir Hills, as well as smaller Precambrian outcrops in the Brahmaputra valley and is elsewhere covered by gently dipping Tertiary beds that reach prodigious thicknesses of several thousand meters in the eastern Himalayan foreland. To calculate the active deformation and inter-seismic motion in shillong plateau, Assam Valley and Mikir hills nineteen campaign

mode of GPS re-measurements were carried out in 2016 (Figure 5.1). Kopili fault separates the Shillong plateau and the Mikir Hills. Two continuous mode Global Positioning System (cGPS) stations (Tezpur, Bomdila) were re-established. These stations are collocated with meteorological sensors. Lumami station maintenance was also carried out.

## 5.6 Active crustal deformation and landslide studies in Garhwal Himalayas

Garhwal Himalayas located in Uttarakhand is one of the most seismically active regions (zone IV and zone V) in the northwestern Himalayas. GPS re-measurements were carried out in 2016 for all the GPS sites in Garhwal Himalayas to estimate the present day active deformation in this region. CSIR-Central Building Research Institute (CBRI) in collaboration with CSIR-4PI has selected two debris type of landslides in Jalgwar village (Chamoli district), Uttarakhand for monitoring. GPS re-measurements were carried out for both the reference and control points in 2016. Operation and Maintenance of Continuous mode Global Navigation Satellite System (CGNSS) in CBRI, Roorkee is carried out and data is streamed in near real time to CSIR-4PI server.

## 5.7 Establishment, operation and maintenance of continuous mode Global Navigation Satellite System (CGNSS) stations

CGNSS stations were established in Chennai and Udupi (Figure 5.3). Udupi station is remotely accessible and sends the data through near real time streaming to the CSIR-4PI servers. CGNSS stations are equipped with geodetic grade dual frequency receivers that can track most of the available GNSS satellites constellations (GPS, GLONASS, Galileo, BeiDou, QZSS). Leh station was re-established (Figure 5.4). Operations and Maintenance of twelve stations in Kashmir valley, Kodaikanal and Hanle GPS station was carried out in 2016-2017. Kodaikanal GPS station is remotely accessible.



Figure 5.3 CGNSS stations established in Chennai and Udupi respectively



Figure 5.4 CGNSS station re-established in Leh

## 5.8 Crustal deformation studies using CGNSS network in Kashmir Valley

The entire Himalayan arc is tectonically active and continues to display seismicity due to active under-thrusting of Indian plate along its boundary. Most of the Himalayan area comes under highly seismic zone area with Kashmir valley classified as zone-V and rest of Jammu and Kashmir classified as zone-IV. Kashmir Valley is located between the Lesser Himalayas (PirPanjal range) and Greater Himalayas. The knowledge presently available on the strain build-up, release and occurrence of earthquake is not adequate enough to assess the seismic vulnerability of this area. CSIR-4PI in collaboration with University of Kashmir, Srinagar has established twelve Continuous mode Global Navigation Satellite System (CGNSS) stations in between 33.5–35° N and 74–76° E in valley along the arc normal transects of Kashmir Himalayas to calculate strain and surface deformation.

CGNSS stations are equipped with geodetic grade dual frequency receivers and observe signals from most of the available GNSS satellites constellations with high sampling rate of 1 Hz.

Data collected from CGNSS network were analyzed in GAMIT/GLOBK software to estimate the crustal deformation. Time series of north, east and up component of the daily position estimates with errors were obtained after data analysis. Time series of Ananthnag CGNSS station is shown in Figure 5.5. Deformation rates calculated over a period of 2 years will provide key input for earthquake hazard mapping of Kashmir valley.

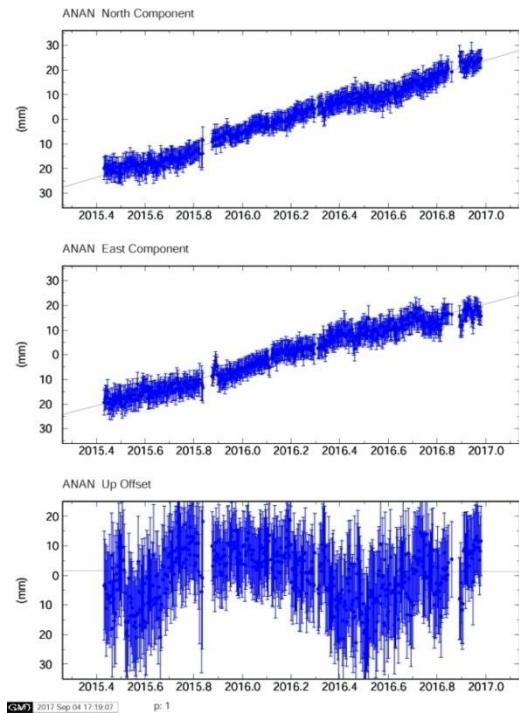


**Figure 5.5 Time Series of Ananthnag CGNSS station**

## 5.9 Landslide mitigation studies in Uttarakhand and north-east India

Uttarakhand and North-East India falls under high risk zone of landslides. Landslide mitigation refers to the techniques used to control the sliding and also reduce the loss of lives and property. Successful landslide mitigation plays a vital role and depends on scientific investigation, construction methods and cost evaluation. Cost effective mitigation measures like vegetation cover, drainage techniques, proper land use measures were studied. Case studies were carried out in landslide prone areas of Gharwal region (Uttarakhand), Assam and Meghalaya to study the simple mitigation techniques. Landslides are caused due to forest fires, improper land measures like building construction without any proper engineering input. Vegetation cover, retaining walls and drainage (surface and sub-surface) techniques are mostly used to control the slides. It is found that mitigation measures were not used in tandem in most of the slide prone areas. Due to

this, the sliding was not effectively controlled which resulted in heavy property losses. Also there is a need to create awareness in public and implement simple mitigation techniques by local community in addition to the government organizations for effective control of landslides.

### **5.10 Seismic hazard and risk assessment based on the Unified Scaling Law for earthquakes: Thirteen principal urban agglomerations of India**

The deterministic seismic hazard map of India with spatially distributed peak ground acceleration (PGA) was used to estimate seismic risk using two data sets of the Indian population - the model population data set and the data set based on India's Census 2011. Four series of the earthquake risk maps of the region based on these two population density sets were cross-compared. The discrepancy of the population data and seismic risks estimation were illuminated for the thirteen principal urban agglomerations of India. The confirmed fractal nature of earthquakes and their distribution in space implies that traditional probabilistic estimations of seismic hazard and risks for cities and urban agglomerations are usually underestimated. The results of the systematic global analysis imply that the recurrence of earthquakes in a region is characterized with USLE:  $\log_{10}N(M, L)=A+B \times (5-M)+C \times \log_{10}L$ , where  $N(M,L)$  - expected annual number of earthquakes of magnitude  $M$  within an area of linear size  $L$ ,  $A$  determines seismic static rate,  $B$  – balance between magnitude ranges, and  $C$  - fractal dimension of seismic loci. We apply the seismic hazard and risk assessment methodology developed recently based on USLE, pattern recognition of earthquake-prone geomorphic nodes, and neo-deterministic scenarios of destructive ground shaking. Objects of risk are individuals (i) as reported in the 2011 National Census data and (ii) as predicted for 2010 by Gridded Population of the World (model GPWv3); vulnerability depends nonlinearly on population density. The resulting maps of seismic hazard and different risk estimates are cross-compared. To avoid misleading interpretations, we emphasize that risk estimates presented here for academic purposes only. In the matter of fact, they confirm that estimations addressing more realistic and practical kinds of seismic risks should involve experts in distribution of objects of risk of different vulnerability, i.e., specialists in earthquake engineering, social sciences, and economics.

### **5.11 Crustal Structure of the Kashmir Basin in NW Himalaya**

A crustal shear wave velocity model for the intermontane Kashmir valley is derived from eight broadband seismic stations located on hard rock sites surrounding and within the valley. Receiver Functions (RFs) at these sites were calculated using the iterative time domain deconvolution and jointly inverted with fundamental-mode, Rayleigh-wave group velocity dispersion data to estimate the underlying shear-wave velocity structure. The inverted Moho depths were further constrained within  $\pm 2$  km by forward modeling. The Moho depth beneath the PirPanjal range in SW of the valley is 57-58 km which further deepens to 60 km along NE with an upwarp of  $\sim 4$  km beneath the valley, not elsewhere reported in the Himalayas. The velocity model developed from this study is further used to relocate the seismicity of the region from period 1964-2015 with better constraints on epicentral and depth location. The obtained velocity model was also employed in

locating ~200 locally recorded events within the valley most of those lie along the valley axis and may represent the starting of locked portion of the decollement beneath the Valley, as also suggested by Global Positioning Studies.

### **5.12 Strong ground motion estimation in NW Himalaya using stochastic finite-fault method**

A stochastic finite fault simulation of ground motion based on dynamic corner frequency is employed to generate Peak Ground Acceleration (PGA) map for NW Himalaya with particular emphasis on Kashmir Himalaya and adjacent areas. Gross features of the ground motion are determined from deterministic parameters like Magnitude, stress drop, strike and dip angles etc. and parameters like rupture velocity and slip are treated as random using random vibration theory. Here a finite fault is considered and is divided into number of subfaults, where each sub-fault is treated as a point source. We used a dynamic corner frequency approach, where rupture begins with a higher  $f_{max}$  and progresses towards lower  $f_{max}$  thus balancing the energy radiated irrespective of the sub-fault size. An analytical method was also used to simulate accurately near-fault ground motions by generating long-period pulses caused by the forward directivity of the rupture. The earthquake catalogue used in this study includes historic events like 1555 Kashmir, 1885 Baramulla events that have been compiled from various sources. All earthquakes of magnitude  $M_w \geq 5.0$  are used in simulation and synthetic seismograms have been generated at a regular grid of  $0.2^\circ \times 0.2^\circ$  and peak values of acceleration at each site were picked. Expected PGA value for Kashmir Basin and Muzaffarabad is  $\approx 0.3-0.5g$  and  $\approx 0.35g$  for Kangra region. The value of PGA estimated here is found to be larger than those estimated by Bureau of Indian Standards. Acceleration time series obtained were further integrated using omega arithmetic integration method to obtain velocity and displacement time series where peak motions were also picked to map. Finally, the obtained PGA map of the region was compared with observed intensities of recent earthquakes and generated acceleration time series were plotted to observe the effect of fault distance and azimuthal variation. This study provides a ground motion database for better design of buildings in the study region from any strong nearby future earthquake(s).

### **5.13 Ambient Noise Tomography of the Kashmir Basin: Cross-correlations of daily waveforms**

Most of the seismic data recorded all over the globe comprises of ambient seismic noise, a rough estimation is that 90-95 % of total data recorded is noise, usually that much data was thrown out till the seismic interferometry was developed to make sense from noise. In early 2000's it was shown experimentally that cross-correlation of ultrasonic waveforms recorded continuously at different locations in a random wave-field shall theoretically be equal to energy recorded at one location if there had been an impulsive seismic source at the other and vice-versa. This was followed by its application in passive seismology to determine the upper structure of crust to which the surface waves are more sensitive. We performed phase weighted cross-correlation of daily

waveforms followed by phase-weighted stacking to further minimize the noise. Unlike time-domain stacking, phase weighted stacking is an amplitude unbiased coherence measure which stacks different traces based on their instantaneous phase at a certain time 't' (say). We estimated such correlation for vertical components of AHR-BAR pair of stations. The correlation is asymmetric with sources mostly lying behind AHR which is also true as nearest ocean lies behind AHR hence reason for strong energy peak at +35 s. Assuming group velocity of ~2 km/s the approximate distance comes to be ~70 km which is close to true inter-station distance of 74.6 km. Further frequency time analysis is used to obtain dispersion curve for fundamental mode phase and group wave velocity. This analysis will be followed for all station pairs ( $n*(n-1)/2$ , where n is number of stations), further a 2D inversion of the dispersion data will be done to see any variation with across latitude and longitude and at different periods.

### **5.14 Earthquake catalogue in north Himalaya for hazard analysis in Jammu & Kashmir**

Jammu & Kashmir region, situated in NW part of Himalaya, has been visited by several damaging earthquakes of magnitude greater than 7.0 which poses a great threat to the millions of people living in the region specially Kashmir valley with 7 million population. Thus, it becomes important to quantify the seismic hazard in the region for future events in terms of possible ground shaking. Comprehensive information of earthquake is required for the estimation of hazard in the region. Earthquake catalogue has been generated for Jammu & Kashmir region (28° to 38° and 71° to 83°) using from various sources including USGS, ISC, GEM, IMD etc. and the historic catalog. Generally, instrumental and most accurate data is available after 1960 from ISC, from USGS since 1973 and IMD. Data from 1920 – 1960 is available in International Seismological Summary reports. ISC-GEM also provides earthquake data for the period 1900 to 2013 for the magnitude > 5.0. For historical data we used catalog from published literature work and converted intensities into magnitude and the catalog it is listed by NOAA. After collection of the earthquake data from various sources, it has been merged and cleaned up for duplicate reporting of events from different sources. Regression relations have been established using orthogonal regression method on Harvard CMT data to establish various magnitude conversion relations and all magnitude converted to Moment magnitude ( $M_w$ ) for the J & K catalogue.

### **5.15 Receiver function interpolation computation for central Himalaya**

In order to estimate shear velocity model of the Kumaon-Garhwal Himalaya, 57 seismic stations has been used from three experiments in this region: 1) the 2005-2008 National Geophysical Research Institute (NGRI) deployment (UT), 2) the 2007-2008 Wadia Institute of Himalayan Geology (WIHG) 3) the 2007-20011 US-China West Tibet array (Y2) .

Receiver function represent  $P_s$  conversions corresponding discontinuities, beneath the seismic station, along with its multiples ( $P_pP_m$ s and  $P_pS_m$ s). Receiver functions are obtained by deconvolving vertical component from radial and transverse component to remove source and

instrument effect. In this study, receiver functions are computed using time domain iterative deconvolution method. Earthquake waveform from all 57 stations are used to compute receiver functions using events with recorded magnitude  $M_w \geq 5.7$ , at epicentral distances between  $30^\circ$  and  $100^\circ$ . A Gaussian of width 1.0 and 1.6 was used in the deconvolution. After deconvolution, those receiver functions which retrieved less than 85% of the original radial component (after convolving with vertical component) were rejected. A handful of remaining outlier is removed during visual inspection. A total 18430 receiver functions were computed and 5573 receiver functions (~ 30 %) are selected for further analysis. Usually receiver functions are stacked from similar azimuth and distances to reduce the noise and then inverted for shear wave velocities. Instead, in this study, receiver function interpolation is used to construct wavefield for the region to obtain smooth and simplified P wave receiver functions.

In interpolation approach, first, all available receiver function measurement are binned into three parameter ranges, correspond to values larger than 0.07 s/km, between 0.05 and 0.07 s/km and smaller than 0.05 s/km respectively. For each ray parameter the RF at each station is computed from a weighted average of all the station waveforms with in the specific distance,  $d_2$ , from the location of interest (LOI). Weight for signals recorded within a distance  $d_1$  was 1.0, while those located between the distance  $d_1$  and  $d_2$  of the LOI decreased linearly from 1.0 to 0.0 across the range from  $d_1$  to  $d_2$ . An interpolated RF was computed by summing the weighted, binned Rfs and normalized by the sum of the weights. The distance range can be chosen considering the station spacing and the amount of smoothing desired. When we increase interpolation parameters ( $d_1$  and  $d_2$ ) RFs become smooth as it suppress shallow and localized structure response. For creating a complete 3D shear wave structure for the region, we have divided region into 154 cells as grid and computed interpolated RFs for the all 154 locations as cells.

## **5.16 Site characterization of Srinagar city, Kashmir valley, Northwest Himalaya H/V spectral ratio method**

Kashmir Basin is a seismically active basin due to its out-of-sequence thrust faulting and tectonically active adjoining areas. Its geomorphology, structure and lateral extent indicate significant accommodation of stress since long, which is further supported by the absence of a large earthquake in this region and also evident from seismically quiescent region between 2005 Kashmir and 1905 Kangra earthquakes. Most destructive earthquakes are associated with strong seismic ground motion and seismic wave amplification due to local site effects, particularly in the basins. With this view, we undertook the task of site-specific seismic microzonation study, which is the process of estimating the fundamental mode frequency, response of soil layers and its classification. Microtremor Survey has been carried out in the Srinagar city (having more than 1.8 million inhabitants) and its peripherals by making a grid of 300 by 300 meters, hence approx. 300 sites location were chosen to record the ambient vibrations. We deployed a Lennartz seismometer (5 s period) and a City Shark-II data acquisition system to acquire ambient noise in forms of three components, viz. NS, EW, and vertical directions. The ratio between the Fourier amplitude spectra of the horizontal to the vertical (H/V) components of persisting Rayleigh waves were calculated from the ambient noise vibrations acquired from the first 40 stations using the GEOPSY software.

The H/V spectral ratios were plotted between 0.2 and 25 Hz encompassing the complete range of resonating frequencies recorded within the study area. The preliminary results show the significant variation in fundamental frequencies that means the region is quite heterogeneous and geologically complex in terms of soft soil deposits. That will implicate towards uneven amplification pattern in case of the occurrence of any major earthquake. This will be a first site-specific seismic hazard study in Srinagar city and in turn will be helpful assessing the part of damage in populated and urban areas of Srinagar city.

### **5.17 Subsurface profiling along Banni plains and bounding faults, Kachchh, Western India using microtremors method**

The present article is a maiden attempt to map shallow subsurface rheological interfaces laterally across Banni plains and decode geometry of antecedent fault associated with Kachchh Mainland Fault (KMF) using the microtremor method. Microtremor measurements were carried out at 31 sites along N-S transect from Loriya in Mainland Kachchh to Birandhiyara in Patcham Island across Banni plains. We applied H/V spectral ratio technique to estimate the fundamental resonant frequencies at each site and considered for interpretation. The results show presence of two distinct rheological interfaces designated by frequencies 0.23 Hz to 0.29 Hz and 0.8252 Hz to 1.5931 Hz. These frequencies are compared with depths of Mesozoic-Basement (M-B) interface and Quaternary-Tertiary (Q-T) interface. The velocity for Rayleigh waves calculated for M-B and Q-T interfaces are 1830 m/s and 411 m/s respectively. The depths for sites are calculated using both  $V_s$  as well as the standard non-linear regression relationship ( $h = 110.18f_r^{-1.97}$ ) derived for Banni plains. The depths for M-B and Q-T vary from 1442-1965 m and 44-160 m, respectively. The subsurface profile across Banni plains educe cluster of four faults that develop an array of imbricate faults in forefront of Kachchh Mainland Fault within Banni Footwall. The geometry of faults together suggest a 'positive flower structure' indicating step-over's, strain restraining bends displaying push-ups due to localized shortening between converging bends of KMF and SWF. Banni Footwall Syncline preserves evidence of two episodes of deformations. The initial deformation event led to subsidence within Kachchh Mainland Fault Zone bringing Mesozoic sequence juxtaposed against basement rocks, whereas the later event led to development of a positive flower structure in the Kachchh Mainland Fault Zone. The present study provides an opportunity to sense fault and fault geometry bridging surfaces structural grains with deep crustal structures.

### **5.18 Subsurface profiling of granite pluton using micro tremor method: southern Aravalli, Gujarat, India**

We report, using the micro tremor method, a sub-surface granitic pluton underneath the Narukot Dome and in its western extension along a WNW profile, in proximity of eastern fringe of Cambay Rift, India. The present finding elucidates development of an asymmetric double plunge along Narukot Dome. Micro tremor measurements at 32 sites were carried out along the axial trace (N95°) of the dome. Fourier amplitude spectral studies are applied to obtain the ratio between the

horizontal and vertical components of persisting Rayleigh waves as local ambient noise. Fundamental resonant frequencies for each site are considered to distinguish sediment discontinuity boundary. Two distinct rheological boundaries are identified based on frequency ranges determined in the terrain: (i) 0.2219-10.364 Hz recorded at 31 stations identified as the Champaner meta-sediment and granite boundary, and (ii) 10.902-27.1119 Hz recorded at 22 stations identified as the phyllite and quartzite boundary. The proposed equation describing frequency-depth relationship between granite and overlaying regolith is in agreement to those already published in literature. The morphology of granite pluton highlights the rootless character of Champaner Group showing sharp discordance with granitic pluton. The findings suggest manifestation of pluton at a shallower depth implies a steep easterly plunge within Champaner metasediments, whereas signature of pluton at a deeper level implies a gentle westerly plunge. The present method provides an opportunity to assess the role of granite emplacement in influencing the surface structural grain as well as characterizing subsurface Precambrian terrain and their association with mineral resources.

### **5.19 A study on Progressive Collapse behaviors' of steel and RCC moment frames**

One of the key requirements for any major construction is the structural safety of the building along with the ability to resist partial or total collapse. One or more structural elements fail due to abnormal loading, leading to the collapse of the entire structure progressively. This phenomenon is referred to as Progressive Collapse. Seismic loading may also cause progressive collapse of the structure due to repeated lateral loading on a critical load-bearing element in a building in seismically prone regions. The capacity of a building has been analyzed to resist collapse of 15 storey 3D Steel and RCC moment resisting frames using the Linear Static method and Linear Time history method of analysis. The building has been modeled and designed for seismic zone 5 as per Indian Standards using ETABS. Three scenarios of column removal namely middle, corner and interior has been studied to arrive at the most critical location of column loss. The Demand Capacity Ratio (DCR) has been assessed in the critical regions as per the provisions of GSA guidelines. Further, the variation in the maximum vertical displacement values for both the steel and RCC structures has been compared. The study concludes that the loss of column in the corner location proved more susceptible to collapse by comparing the DCR values. It has also been observed that a steel building that has been designed to resist seismic loads corresponding to zone 5 has the ability to resist collapse following the loss of a column when compared to an RCC building. Further, a 20 storey building showed lower displacement values indicating that is less susceptible to progressive collapse when compared to a 10 or 15 storey building. The effect of two methods firstly increasing the beam size and secondly providing bracings to enhance the response of the RCC moment resisting framed structure was investigated. The increase in the beam size did not bring about any reduction in the DCR values in the lower storey levels. However, the provision of bracings proved effective in drastically reducing the DCR as well as vertical displacement values.

## **5.20 Study on special truss moment frames and special moment resisting frames with fluid viscous dampers as a seismic retrofit**

Earthquakes can cause profound damage to various structures depending on its magnitude. To improve the seismic resistance of existing structures, seismic retrofitting needs to be done. Installation of Fluid Viscous Dampers (FVDs) is one such seismic retrofitting technique. Steel structures are known to perform better under seismic action than any other material due to their flexibility and low weight. The objective of this study is to investigate the effects of Fluid Viscous Dampers (FVDs) on the seismic response of a structure. This study includes seismic retrofit of FVDs to Special Moment Resisting Frames (SMRFs) and Special Truss Moment Frames (STMFs) and comparison of their behavior. A 15 storey structure is considered in this study which is modeled in the ETabs software. The diagonal bracing system is considered for the damper configuration. The structures i.e., the bare frames and the retrofitted frames are subjected to linear time history analysis. Parameters such as lateral top displacement and energy dissipation behavior are studied for the bare and retrofitted frame and comparisons are drawn. A comparison is also drawn of the seismic behavior between the SMRF and STMF. Results indicate that the Fluid Viscous Damper significantly reduces the effects due to an earthquake and is an effective retrofit against seismic action for SMRFs. However, the FVDs only marginally improve the seismic performance of STMFs. It is also observed that the STMFs perform much better than the SMRFs as far as structural deformation goes. The energy dissipation behavior is also found to be improved with the addition of FVDs in case of SMRFs and is unaffected in case of STMFs. Hence, the study concludes that the STMFs outperform the SMRFs with respect to seismic resistance and that the Fluid Viscous Dampers can be used as an effective seismic retrofit only in case of Special Moment Resisting Frames.

## **5.21 Study on P-delta effects of a building with soft storey**

In modern multi-storey buildings stiffness irregularities are usually found within the building that may be due to the occupancy and architectural appearance. Such irregularities in elevation can lead to buildings with soft stories. Soft story refers to the existence of a building floor that presents a significantly lower stiffness than the others. As per IS1893 (part 1) – 2002, in a soft storey lateral stiffness of the storey is less than 70% of the above storey or less than 80% of the average lateral stiffness of the above three stories. Usually open soft storey is provided at ground level to accommodate parking, reception lobbies etc. also, the soft storey may be constructed at the intermediate level for the purpose such as offices, function halls, supermarkets etc. Such soft storey configuration may lead to serious earthquake damage. To experience minimum damage and less psychological fear in the minds of people during the earthquake, IS1893 (part1):2002, permits maximum inter-storey drift as 0.004 times the storey height. Inter storey drift always depends upon the stiffness of the respective storey. To understand the behavior of P-delta effects different types of 20storey buildings are modeled using ETABS software and subjected to earthquake loading. Building parameters are varied by introducing shear wall, exterior walls,

bracing system and further parameters such as storey drift, roof displacement and column moments are computed and variations in these parameters are discussed and it is observed that building with open soft storey has the least capacity to resist failure during earthquake.

## **5.22 Dynamic analysis to compare buckling restrained braces and conventional braces in RC frames**

The building structure should possess requisite strength and stiffness to resist the gravity loads and the lateral loads. To limit deflections, the structure should also possess vertical and lateral stiffness. A good lateral resisting structural system is one, which behaves in elastically by having greater redundancy thereby having larger ductility and damping. In addition to the strength and stiffness of the structure, architectural considerations often dictate the type of structural system to be chosen. So engineers are required to choose the appropriate type structural system, which is able to resist the lateral forces along with the gravity loads within functional and architectural constraints. There are many types of lateral load resisting systems in practice, special moment resisting frame (SMRF), shear wall structure, braced frame, frame tube system, outrigger frame, coupled shear wall and dual system. In the present study, 15 storey RC frames of storey height 3m with two bay widths 6m and 8m are modeled to compare between BRB and conventional steel braces considering chevron and X configuration arranged in corner and center bay locations. For the purpose of comparison dynamic analysis which includes response spectrum and linear time history analysis are performed on all the frames and the parameters such as modal time period, base shear and displacement are considered. The analysis is performed using commercially available software ETABSv2016. From the analysis of results, the better performing bracing system, better configuration and location of bracings are studied. Also the difference in variation between two bracing systems from 6m bay width frame to 8m bay width frame is studied.